Delay-Dependent Stability for Load Frequency Control With Constant and Time-Varying Delays

L. Jiang, *Member, IEEE*, W. Yao, Q. H. Wu, *Fellow, IEEE*, J. Y. Wen, and S. J. Cheng, *Fellow, IEEE*

***Abstract*—Load frequency control (LFC) requires transmitting measurements from remote RTUs to control center and control signals from the control center to plant side. Constant delays exist in the conventional dedicated communication channels, while the future usage of open communication networks will introduce time-varying delays. Those delays would degrade the dynamic performance of LFC and in the worst case, cause instability. The maximal delay time which allows an LFC scheme embedded with controllers to retain stable is defined as the delay margin. This paper investigates the delay-dependent stability of the LFC scheme by using Lyaponuv-theory based delay-dependent criterion and linear matrix inequalities (LMIs) techniques. Case studies are carried out based on one-area and multi-area LFC schemes installed with proportional-integral (PI) controllers, respectively. Relationship between the gains of PI controller and the delay margin of the LFC scheme are investigated and results obtained can be used to tune the PI controllers to achieve a compromise between the dynamic performance and the delay margin. Both constant and time-varying delays are considered. The effectiveness of the criterion used is verified by simulation studies.**

***Index Terms*—Constant time delay, delay margin, delay-dependent stability, load frequency control, time-varying delay.**

I. Introduction

LOAD frequency control (LFC) has been used effectively in power systems for many years [1], [3], [23]. Its basic objective is to restore the balance between load and generation in each control area. In conventional LFC schemes, dedicated communication channels are used for transmission of measurements from remote RTUs to the control center and control signals from the control center to the generator unit [2], [3]. Although there is a constant delay introduced, such a delay is always ignored during the design and operation of the LFC. When a communication fault happens, a fault counter will be triggered to record the fault period. The LFC scheme will be suspended or stopped when the counted steps reach the predefined upper bound. This upper bound is usually chosen as a conservative small value based on operational experience [1]. The data drop caused by the communication fault can be converted to an equivalent time-varying delay.

A major challenge for the power system under deregulation and market environment is to integrate computing, communication, and control into appropriate levels of system operation and control, as indicated by Bose in 2005 [4]. This trend will be enhanced by the currently developing of smart grid technologies in which communication networks provide a backbone of the integration of the information technologies and the power systems. An effective power system market highly needs an open communication infrastructure to support the increasing decentralized property of control services such as LFC [5], [7], [23], [24]. The open communication infrastructure will also allow a bilateral contract for the provision of load following and third party LFC. Under this case, a certain part of generator units will receive a control signal to increase or reduce the power output, from either a control center or from the customer side directly. With the introduction of open communication channel, both constant and time-varying delays will be introduced in the LFC scheme [5].

LFC scheme equipped with communication channels is a typical time delay system. From stability analysis and controller design point of view, it is very important to find the maximal delay which allows an LFC scheme embedded with controllers to retain stable. This maximal delay is defined as a delay margin for stability analysis. Recently, time delays have been considered in the design of load frequency controller in a deregulation and market environment [6]–[13]. Among those works, some of them did not consider the time delay at the design stage [6], [7], [25], [26], and most of them employed a robust control method in which the time delay is dealt as part of uncertainties [8]–[13]. However, the effectiveness of proposed controller against time delay was always verified by simulation studies only, while the determination of delay margin for LFC scheme has not been reported yet.

There are mainly two kinds of methods to determine the delay margin of time delay system, with different level of limitations and conservativeness. One is the direct methods, such as tracing critical eigenvalue [14] and cluster treatment of characteristic roots [15]–[17]. Those direct methods can provide the accurate delay margin by calculating eigenvalues of whole system. As the detailed system model is required, those methods are time consuming when the size of system increased. Those two direct

Manuscript received May 16, 2011; revised September 03, 2011; accepted October 05, 2011. Date of publication November 14, 2011; date of current version April 18, 2012. This work was supported in part by the National Natural Science Foundation of China (Grant no. 50937002 and 51071185) and in part by the Research Support Fund of the University of Liverpool. Paper no. TPWRS-00384-2011.

L. Jiang and Q. H. Wu are with the Department of Electrical Engineering and Electronics, University of Liverpool, Liverpool L69 3GJ, U.K. (e-mail: ljiang@liv.ac.uk; qhwu@liv.ac.uk).

W. Yao is with the State Key Laboratory of Advanced Electromagnetic Engineering and Technology, Huazhong University of Science and Technology, Wuhan 430074, China, and was with the Department of Electrical Engineering and Electronics, The University of Liverpool, Liverpool L69 3GJ, U.K. (e-mail: yao_wei@163.com).

J. Y. Wen and S. J. Cheng are with the State Key Laboratory of Advanced Electromagnetic Engineering and Technology, Huazhong University of Science and Technology, Wuhan, 430074, China (e-mail: jywen@hust.edu.cn; sjcheng@hust.edu.cn).

Digital Object Identifier 10.1109/TPWRS.2011.2172821

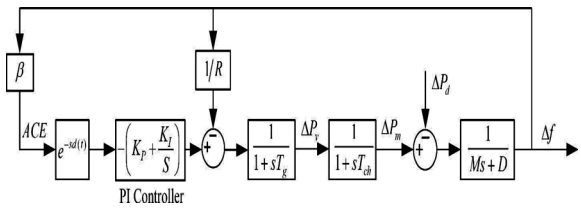

Fig. 1. Dynamic model of one-area LFC scheme.

calculation methods can obtain the accurate delay margin; however, they can only deal with constant time delays. The other is an indirect method based on Lyapunov stability theory and linear matrix inequalities (LMIs) techniques [18]–[20] and has been applied to calculate the delay margin of the wide-area damping controller [22]. Although these methods have some conservativeness, they can deal with both constant and time-varying delays.

This paper investigates the delay-dependent stability of an LFC scheme considering constant and time-varying delays. The method used is based on delay-dependent criterion with a single time delay proposed in [19] and with multiple time delays proposed in [21]. At first, one-area and multi-area LFC schemes equipped with PI controller are modified to include time delays. After recalling the delay-dependent criterion, the delay margins of LFC scheme are determined and the relationship between delay margin and gains of PI controller is investigated. Case studies are based on one-area and multi-area LFC schemes, respectively. Simulation studies are performed to verify the effectiveness of the criterion used.

II. Dynamic Model of LFC With Delay

The model of conventional LFC scheme is modified to include the time delay into the control loop, for one-area LFC scheme and multi-area LFC scheme, respectively[1], [23] . All generators are assumed to be equipped with non-reheat turbine. Other types of turbine, such as reheat turbine and hydro turbine, can be modeled in a similar way and not presented. A PI controller, which is the load frequency controllers used currently in industry, is included in the model.

A. One-Area LFC Model

The dynamic model of one-area LFC system, shown in Fig. 1, can be expressed as follows[1], [23]:

$$\begin{cases} \dot{\bar{x}}(t) = \bar{A}\bar{x}(t) + Bu(t) + \bar{F}\Delta P_d \\ \bar{y}(t) = \bar{C}\bar{x}(t) \end{cases} \tag{1}$$

where

$$\begin{aligned} \bar{x}(t) &= [\,\Delta f \quad \Delta P_m \quad \Delta P_v\,]^T \\ \bar{y}(t) &= ACE, \\ \bar{A} &= \begin{bmatrix} -\frac{D}{M} & \frac{1}{M} & 0 \\ 0 & -\frac{1}{T_{ch}} & \frac{1}{T_{ch}} \\ -\frac{1}{RT_g} & 0 & -\frac{1}{T_g} \end{bmatrix} \\ \bar{B} &= \begin{bmatrix} 0 & 0 & \frac{1}{T_g} \end{bmatrix}^T \\ \bar{F} &= [\,-\tfrac{1}{M} \quad 0 \quad 0\,]^T \\ \bar{C} &= [\,\beta \quad 0 \quad 0\,] \end{aligned}$$

and Δf, ΔP_m, ΔP_v, and ΔP_d are the deviation of frequency, the generator mechanical output, valve position, and load, respectively. M, D, T_g, T_{ch}, and R denote the moment of inertia of the generator, generator damping coefficient, time constant of the governor, time constant of the turbine, and speed drop, respectively.

Due to no net tie-line power exchange in the one-area LFC scheme, the area control error ACE is defined as

$$ACE = \beta\Delta f \tag{2}$$

where β is frequency bias factor. For simplicity, delay existing at the transmission of control signal between the control center and the plant is aggregated with the delay existing in the transmission of ACE, as shown by an exponential block $e^{-sd(t)}$ in Fig. 1. Using ACE as the input of load frequency controller, a PI controller is designed as

$$u(t) = -K_P ACE - K_I \int ACE \tag{3}$$

where $K = [\,K_P \quad K_I\,]$, K_P and K_I are proportional and integral gains, respectively; $d(t)$ denotes the time-varying delay.

In order to simplify the analysis, the PI control problem is transformed into a static output feedback (SOF) control problem [10], [11]. Define the following new virtual state and measurement output vectors:

$$\begin{aligned} x(t) &= [\,\Delta f \quad \Delta P_m \quad \Delta P_v \quad \int ACE\,]^T \\ y(t) &= [\,ACE \quad \int ACE\,]^T \end{aligned}$$

and apply the PI controller (3) into system (1), the closed-loop model of one-area LFC system can be expressed as follows:

$$\begin{cases} \dot{x}(t) = Ax(t) + A_d x(t - d(t)) + Bu(t) + F\Delta P_d \\ y(t) = Cx(t) \end{cases} \tag{4}$$

where

$$\begin{aligned} A &= \begin{bmatrix} -\frac{D}{M} & \frac{1}{M} & 0 & 0 \\ 0 & -\frac{1}{T_{ch}} & \frac{1}{T_{ch}} & 0 \\ -\frac{1}{RT_g} & 0 & -\frac{1}{T_g} & 0 \\ \beta & 0 & 0 & 0 \end{bmatrix} \\ A_d &= \begin{bmatrix} 0 & 0 & 0 & 0 \\ 0 & 0 & 0 & 0 \\ -\frac{K_P\beta}{T_g} & 0 & 0 & -\frac{K_I}{T_g} \\ 0 & 0 & 0 & 0 \end{bmatrix} \\ B &= \begin{bmatrix} 0 & 0 & \frac{1}{T_g} & 0 \end{bmatrix}^T \\ F &= [\,-\tfrac{1}{M} \quad 0 \quad 0 \quad 0\,]^T \\ C &= \begin{bmatrix} \beta & 0 & 0 & 0 \\ 0 & 0 & 0 & 1 \end{bmatrix}. \end{aligned}$$

$\int ACE$ is integration of the area control error ACE. Note that the output $y(t)$ in above model is just a virtual vector and the practical measurement output is ACE.

B. Multi-Area LFC Model

For a multi-area LFC scheme, all generation units in each control area are simplified as an equivalent generation unit. As

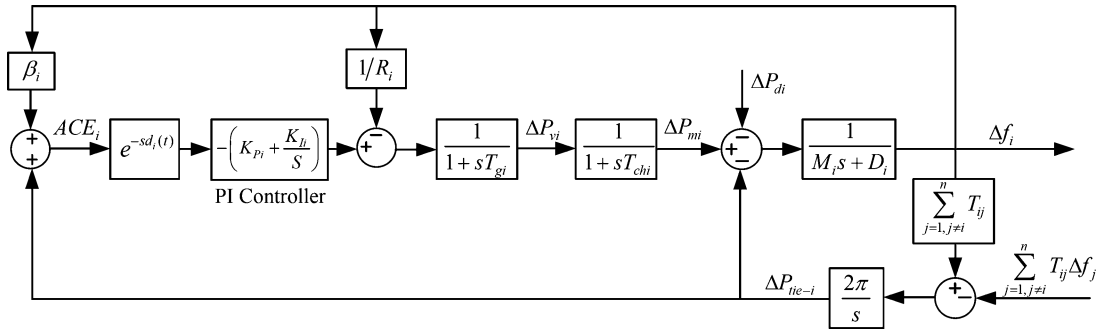

Fig. 2. Dynamic model of the ith control area in a multi-area LFC scheme.

shown in Fig. 2, dynamic model of the multi-area power system including n control areas can be obtained as follows [1], [23] :

$$\begin{cases} \dot{x}(t) = Ax(t) + Bu(t) + F\Delta P_d \\ y(t) = Cx(t) \end{cases} \tag{5}$$

where

$$\begin{aligned}
x_i(t) &= [\,\Delta f_i \quad \Delta P_{mi} \quad \Delta P_{vi} \quad \int ACE_i \quad \Delta P_{\mathrm{tie}i}\,]^T \\
y_i(t) &= [\,ACE_i \quad \int ACE_i\,]^T \\
x(t) &= [\,x_1(t) \quad x_2(t) \quad \cdots \quad x_n(t)\,]^T \\
y(t) &= [\,y_1(t) \quad y_2(t) \quad \cdots \quad y_n(t)\,]^T \\
u(t) &= [\,u_1(t) \quad u_2(t) \quad \cdots \quad u_n(t)\,]^T \\
\Delta P_d(t) &= [\,\Delta P_{d1}(t) \quad \Delta P_{d2}(t) \quad \cdots \quad \Delta P_{dn}(t)\,]^T \\
A &= \begin{bmatrix} A_{11} & A_{12} & \cdots & A_{1n} \\ A_{21} & A_{22} & \cdots & A_{2n} \\ \vdots & \vdots & \ddots & \vdots \\ A_{n1} & A_{n2} & \cdots & A_{nn} \end{bmatrix} \\
B &= diag\,[\,B_1 \quad B_2 \quad \cdots \quad B_n\,] \\
C &= diag\,[\,C_1 \quad C_2 \quad \cdots \quad C_n\,] \\
F &= diag\,[\,F_1 \quad F_2 \quad \cdots \quad F_n\,] \\
B_i &= \left[0 \quad 0 \quad \tfrac{1}{T_{gi}} \quad 0 \quad 0\right]^T \\
F_i &= \left[-\tfrac{1}{M_i} \quad 0 \quad 0 \quad 0 \quad 0\right]^T \\
C_i &= \begin{bmatrix} \beta_i & 0 & 0 & 0 & 1 \\ 0 & 0 & 0 & 1 & 0 \end{bmatrix} \\
A_{ii} &= \begin{bmatrix} -\frac{D_i}{M_i} & \frac{1}{M_i} & 0 & 0 & -\frac{1}{M_i} \\ 0 & -\frac{1}{T_{chi}} & \frac{1}{T_{chi}} & 0 & 0 \\ -\frac{1}{R_i T_{gi}} & 0 & -\frac{1}{T_{gi}} & 0 & 0 \\ \beta_i & 0 & 0 & 0 & 1 \\ 2\pi\sum_{j=1,j\neq i}^{n} T_{ij} & 0 & 0 & 0 & 0 \end{bmatrix} \\
A_{ij} &= \begin{bmatrix} 0 & 0 & 0 & 0 & 0 \\ 0 & 0 & 0 & 0 & 0 \\ 0 & 0 & 0 & 0 & 0 \\ 0 & 0 & 0 & 0 & 0 \\ -2\pi T_{ij} & 0 & 0 & 0 & 0 \end{bmatrix} \\
T_{ij} &= T_{ji}
\end{aligned}$$

where T_{ij} is the tie-line synchronizing coefficient between the ith and jth control area. Note that all variables and parameters use the same notation as the one-area LFC scheme plus an additional subscript i.

The ACE signal in a multi-area LFC scheme is defined as follows:

$$ACE_i = \beta_i \Delta f_i + \Delta P_{\mathrm{tie}i} \tag{6}$$

where $\Delta P_{\mathrm{tie}i}$ is the net exchange of tie-line power of the ith control area . The ACE signal combines the area frequency deviation and the net tie-line power exchange is used as the input of the PI controller. For each area, designing a PI controller as (3), the closed-loop model of a multi-area LFC scheme is represented as follows:

$$\dot{x}(t) = Ax(t) + \sum_{i=1}^{n} A_{di}x(t - d_i(t)) + F\Delta P_d \tag{7}$$

where

$$\begin{aligned}
A_{di} &= diag\,[0 \quad \cdots \quad -B_i K_i C_i \quad \cdots \quad 0] \\
K_i &= [\,K_{Pi} \quad K_{Ii}\,] \\
K &= diag\,[\,K_1 \quad K_2 \quad \cdots \quad K_n\,].
\end{aligned}$$

The multi-area LFC scheme has multiple time delays $d_i(t), i = 1 \ldots n$. To simply the analysis and reduce the calculation load of the delay margin for a multi-area LFC scheme, multiple delays are assumed to be equal with each other and represented as a single time delay $d(t)$. Then (7) becomes the same style as(4):

$$\dot{x}(t) = Ax(t) + A_d x(t - d(t)) + F\Delta P_d \tag{8}$$

where $A_d = \sum_{i=1}^{n} A_{di}$.

For a multi-area LFC scheme, the net tie-line power exchange between each control area satisfies the following equation:

$$\sum_{i=1}^{n} \Delta P_{\mathrm{tie}i} = 0. \tag{9}$$

According to (9), state $\Delta P_{\mathrm{tie}i}$ of (8) can be represented by other state variables so as to reduce the order of system(8) by one.

III. Delay-Dependent Stability Analysis Method

The delay-dependent criterion for linear systems with time-varying delay proposed in [19] is used to determine the delay margin of power system with an LFC scheme embedded. The study of stability of system with time delay has been investigated extensively at the control society. In a delay-dependent

system, asymptotic stability holds for $\tau < \tau_d$, where τ denotes the delay and τ_d is a critical delay denoted as a delay margin; and the system is unstable for $\tau > \tau_d$. The τ_d is an important parameter for evaluating the stability of the delay-dependent system.

This section will recall a delay-dependent criterion proposed in [19] which can deal with a linear system with single constant and time-varying delays and an extended delay-dependent criterion proposed in [21] which can deal with a linear system with multiple time delays. The detailed description of those two criterions are shown as follows.

A. Delay-Dependent Stability Criterion for Linear System With Single Time Delay

Consider a nominal system with time-varying delay given by

$$\begin{cases} \dot{x}(t) = Ax(t) + A_d x(t - d(t)) \; t > 0 \\ x(t) = \Phi(t) \; t \in [-\tau, 0] \end{cases} \tag{10}$$

where $x(t) \in R^m$ is the state vector, the time delay, $d(t)$, is a time-varying continuous function that satisfies

$$0 \le d(t) \le \tau, \; \dot{d}(t) \le \mu \le 1 \tag{11}$$

where τ and μ are the upper bound and the varying rate of time delay and both of them are constants; the initial condition, $\Phi(t)$, is a continuous vector valued with initial function of $t \in [-\tau, 0]$. As shown in the following theorem, the delay margin can easily be determined by solving the corresponding LMIs.

Theorem 1: Given scalars $\tau > 0$ and $\mu < 1$, the nominal system (10) is asymptotically stable if there exist symmetric positive-definite matrices $P = P^T > 0$, $Q = Q^T > 0$, and $Z = Z^T > 0$, a symmetric semi-positive-definite matrix $X = \begin{bmatrix} X_{11} & X_{12} \\ X_{12}^T & X_{22} \end{bmatrix} \ge 0$, and any appropriately dimensioned matrices Y and T such that the following LMIs are true:

$$\Phi = \begin{bmatrix} \Phi_{11} & \Phi_{12} & \tau A^T Z \\ \Phi_{12}^T & \Phi_{22} & \tau A_d^T Z \\ \tau Z A & \tau Z A_d & -\tau Z \end{bmatrix} < 0 \tag{12}$$

$$\Psi = \begin{bmatrix} X_{11} & X_{12} & Y \\ X_{12}^T & X_{22} & T \\ Y^T & T^T & Z \end{bmatrix} \ge 0 \tag{13}$$

where $\Phi_{11} = PA + A^T P + Y + Y^T + Q + \tau X_{11}$, $\Phi_{12} = PA_d - Y + T^T + \tau X_{12}$, $\Phi_{22} = -T - T^T - (1-\mu)Q + \tau X_{22}$.

Theorem 1 can be extended to a system with multiple time delays as follows:

$$\begin{cases} \dot{x}(t) = Ax(t) + \sum_{i=1}^{n} A_i x(t - \tau_i) \; t > 0 \\ x(t) = \Phi(t) \; t \in [-\tau, 0] \end{cases} \tag{14}$$

where $x(t) \in R^m$ is the state vector, $\tau_i \ge 0 (i = 1, 2, \ldots, n)$ are constant time delays, $\tau = \max\{\tau_1, \tau_2, \ldots, \tau_n\}$ and $A_i \in R^{m \times m} (i = 1, 2, \ldots, n)$ are constant matrices. The initial conditions, $\Phi(t)$, denote a continuous vector-valued initial function of $t \in [-\tau, 0]$.

For convenience, it is assumed that in(14)

$$0 = \tau_0 \le \tau_1 \le \tau_2 \le \cdots \le \tau_n. \tag{15}$$

Hence, the following Theorem 2 can be deduced from the above assumptions [21].

Theorem 2: For given scalars $\tau_i \ge 0 (i = 1, 2, \ldots, n)$ that satisfy (15), the system (14) with multiple time delays is asymptotically stable if there exist symmetric positive definite matrices $P = P^T > 0$ and $Q_i = Q_i^T > 0 (i = 1, 2, \ldots, n)$, symmetric semi-positive definite matrices

$$X^{ij} = \begin{bmatrix} X_{00}^{ij} & X_{01}^{ij} & \cdots & X_{0n}^{ij} \\ [X_{01}^{ij}]^T & X_{11}^{ij} & \cdots & X_{1n}^{ij} \\ \vdots & \vdots & \ddots & \vdots \\ [X_{0n}^{ij}]^T & [X_{1n}^{ij}]^T & \cdots & X_{nn}^{ij} \end{bmatrix} \ge 0 \; (0 \le i < j \le n)$$

and $W^{ij} = [W^{ij}]^T \ge 0 \; (0 \le i < j \le n)$ and any matrices $N_l^{ij} \; (l = 0, 1, 2, \ldots, n, \; 0 \le i < j \le n)$ such that the following LMIs hold for $0 \le i < j \le n$:

$$\Xi = \begin{bmatrix} \Xi_{00} & \Xi_{01} & \cdots & \Xi_{0n} \\ \Xi_{01}^T & \Xi_{11} & \cdots & \Xi_{1n} \\ \vdots & \vdots & \ddots & \vdots \\ \Xi_{0n}^T & \Xi_{1n}^T & \cdots & \Xi_{nn} \end{bmatrix} < 0 \tag{16}$$

$$\Gamma^{ij} = \begin{bmatrix} X_{00}^{ij} & X_{01}^{ij} & \cdots & X_{0n}^{ij} & N_0^{ij} \\ [X_{01}^{ij}]^T & X_{11}^{ij} & \cdots & X_{1n}^{ij} & N_1^{ij} \\ \vdots & \vdots & \ddots & \vdots & \vdots \\ [X_{0n}^{ij}]^T & [X_{1n}^{ij}]^T & \cdots & X_{nn}^{ij} & N_n^{ij} \\ [N_0^{ij}]^T & [N_1^{ij}]^T & \cdots & [N_n^{ij}]^T & W^{ij} \end{bmatrix} \ge 0. \tag{17}$$

The detailed elements of the matrix Ξ are shown in Appendix A. The stability region of the system with multiple time delays can be determined by using Theorem 2.

As described in [22], both Theorem 1 and 2 can only provide sufficient condition of stability of system (10) for single delay or (14) for multiple delays for a given μ, respectively, and cannot be used directly to find the delay margin. The function $feasp$ provided in the MATLAB/LMI Control Toolbox [28] is used to check the existence of the delay margin based on LMI constraints given in Theorem 1 or 2. For a given μ, by manually increasing the value of τ and checking the feasibility, the delay margin τ_d which is equal to the maximum τ can be found.

B. Summary of Analysis Steps

Detailed implementation of the method proposed is summarized as the following steps:

Step 1) Obtaining linear model of the LFC scheme excluding the controller. All types of turbines, such as reheat turbine, non-reheat turbine, and hydro turbine, can be modeled.

Step 2) Modeling of the closed-loop linear model with time-varying delay. The LFC scheme including controller is represented as the state space form at first. Then, representing time delays of the measurement signals as one time-varying delay, the closed-loop system including the LFC scheme and controller is modeled as a linear system with time-varying delay.

Step 3) Determining the delay margin. Based on the model obtained in Step 2, the stability of system for a given time delay is determined by using $feasp$ solver described in previous section and binary search algorithm. Preset a search interval starting from τ_s and end at τ_e: $[\tau_s, \tau_e]$, and an accuracy requirement τ_{ac}. Then determine the delay margin by the following steps:

Step 3.1) Set a value of time delay by binary method, i.e., $\tau_{set} = (\tau_s + \tau_e)/2$ and determine the stability of system for this delay τ_{set} by using *feasp* solver;

Step 3.2) Reduce the search interval according to the result, i.e., set $\tau_s = \tau_{set}$ for stable case or set $\tau_e = \tau_{set}$ for unstable case.

Step 3.3) Compare the search interval width $\tau_w = |\tau_e - \tau_s|$ with τ_{ac}. If $\tau_w \geq \tau_{ac}$, go to Step 3.1; else stop the search and output the delay margin $\tau_{\max} = \tau_{set}$.

Step 4) Simulation verification. Based on the detailed model obtained in Steps 1 and 2, simulation method is used to find the delay margin by manually increasing the delay with small increment and observing stability of whole system. The effectiveness of the proposed method and conservativeness of Theorems 1 and 2 (or accuracy of the delay margin obtained) can be verified.

It is worth to point out that the combination of $feasp$ solver and binary search algorithm can obtain the results more quickly than methods proposed in [22].

IV. Case Studies

Case studies are carried out based on one-area and multi-area (two-area and three-area) LFC scheme, respectively. Parameters of these systems are tabulated in Appendix B[1], [8]. The delay margins of each LFC scheme are calculated based on the method proposed at the previous section. Delay margins with respect to different value of gains of PI controllers are obtained for constant and time-varying time delays. Simulation studies are used to investigate how the control performance of LFC scheme is affected by the time delay, and verify the effectiveness and accuracy of the stability criterion used.

A. One-Area LFC Scheme

The delay margin τ_d is calculated by using different sets of gains of PI controller. Integral (I) controller is investigated at first as K_P is usually very small in a real LFC scheme [6]. Results of τ_d with respect to the different K_I and different rate μ are shown in Table I and Fig. 3. It can be found that the τ_d decreases with the increase of K_I for both constant and time-varying delays. For a fixed K_I, τ_d decreases with the increase of the rate μ.

The root locus of the closed-loop one-area LFC scheme with respect to K_I is shown in Fig. 4. It can be found that when the K_I changes from 0.2 to 0.05, the delay margin increases sharply from 6.6915 s to 27.9268 s, while the locations of the complex poles almost do not change. This means that the oscillation mode of the closed-loop system with LFC scheme remains similar. Thus, K_I can be chosen to result in a larger delay margin with a relatively small degradation of the dynamic performance. During the design and tuning of the controller, a trade-off between the delay margin and dynamic performance can be achieved.

Results of delay margins with respect to gains of a PI controller (K_P, K_I) are summarized in Table II and Fig. 5 for constant delays $(\mu = 0)$, Table III and Fig. 6 for time-varying delays $(\mu = 0.9)$, respectively. Results show that a relatively larger τ_d can be obtained under smaller K_P and K_I, and τ_d is reduced sharply for bigger K_P and K_I. For a smaller given $K_I \leq 0.05$, τ_d decreases with the increase of the K_P. For $K_I \geq 0.1$, with

TABLE I
Delay Margin $\tau_d \propto K_I$ (one-area LFC)

	τ_d (s)		
K_I	$\mu = 0$	$\mu = 0.5$	$\mu = 0.9$
0.05	27.9268	24.0781	20.4588
0.10	13.7775	11.8188	9.9300
0.15	9.0560	7.7237	6.3888
0.20	6.6915	5.6696	4.5944
0.40	3.1241	2.5518	1.8116
0.60	1.9104	1.4678	1.0116
1.00	0.8858	0.5280	0.4398

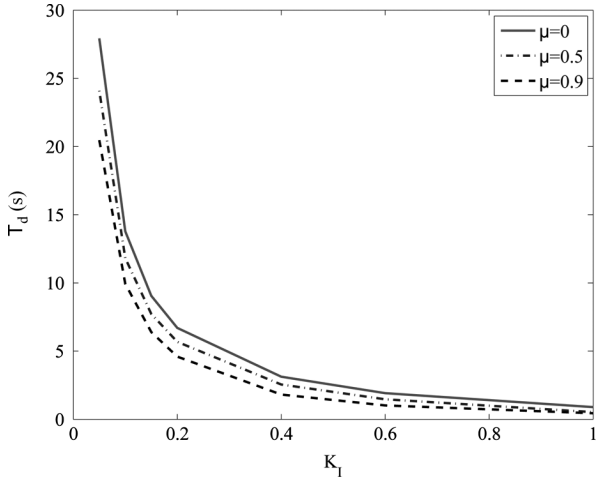

Fig. 3. Delay margin $\tau_d \propto K_I$ (one-area LFC).

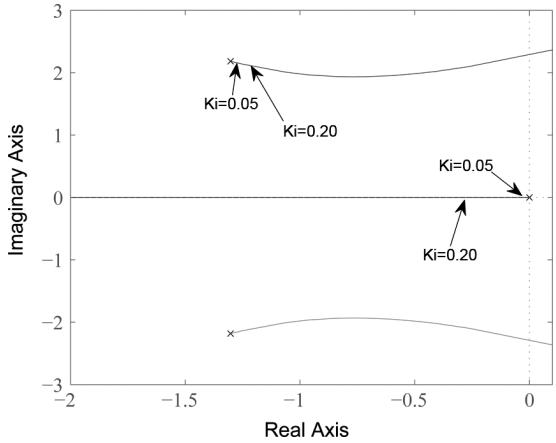

Fig. 4. Root locus of the one-area LFC scheme $(K_P = 0)$.

TABLE II
DELAY MARGIN $\tau_d \propto (K_P, K_I)$ (ONE-AREA LFC, $\mu = 0$)

τ_d (s)	K_I						
K_P	0.05	0.1	0.15	0.2	0.4	0.6	1.0
0	27.927	13.778	9.056	6.692	3.124	1.910	0.886
0.05	27.874	14.061	9.284	6.866	3.215	1.974	0.927
0.10	27.038	13.682	9.220	6.941	3.290	2.029	0.963
0.20	25.114	12.760	8.617	6.535	3.320	2.108	1.016
0.40	20.364	10.426	7.065	5.384	2.832	1.912	1.017
0.60	14.618	7.477	5.1567	3.958	2.130	1.475	0.827
1.00	0.546	0.538	0.530	0.522	0.482	0.438	0.348

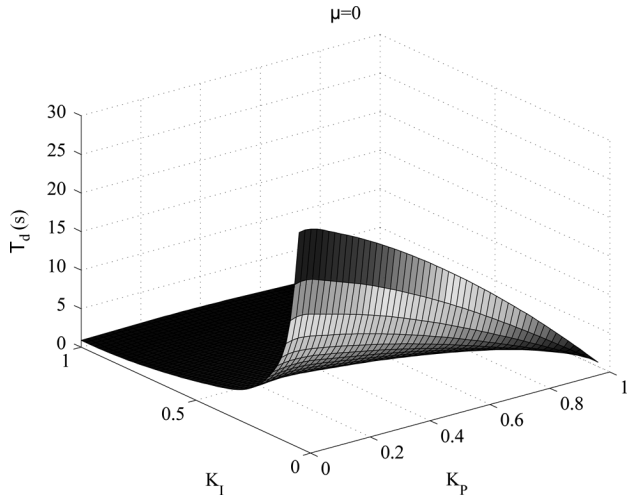

Fig. 5. $\tau_d \propto (K_P, K_I)$ (one-area LFC, $\mu = 0$).

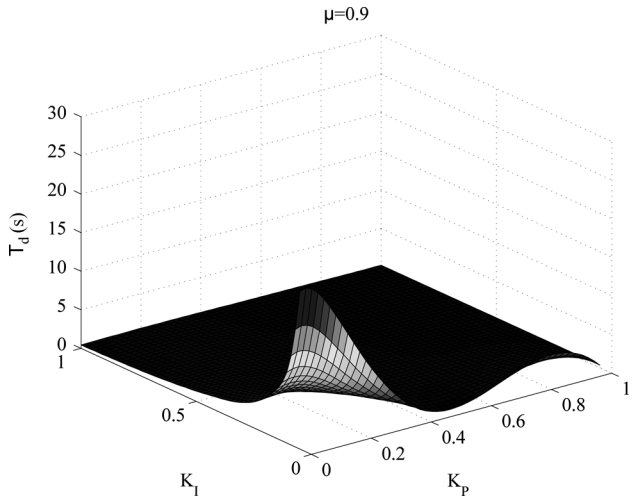

Fig. 6. $\tau_d \propto (K_P, K_I)$ (one-area LFC, $\mu = 0.9$).

the increasing of the value of K_P, τ_d increases at first and then decreases, and the increment of the τ_d become bigger for a larger K_I. That means for a given K_I, there is a range of K_P which can achieve the maximum τ_d. These findings can be used to guide the tuning of PI controllers to achieve the maximal delay margin. Moreover, for same values of (K_P, K_I), the τ_d for the time-varying delays is smaller and reduces much faster than that of the constant delays.

TABLE III
DELAY MARGIN $\tau_d \propto (K_P, K_I)$ (ONE-AREA LFC, $\mu = 0.9$)

τ_d (s)	K_I						
K_P	0.05	0.1	0.15	0.2	0.4	0.6	1.0
0	20.459	9.930	6.389	4.594	1.812	1.012	0.440
0.05	20.031	10.173	6.623	4.769	1.880	1.048	0.468
0.10	17.399	9.164	6.263	4.672	1.854	1.052	0.489
0.20	10.489	5.803	4.149	3.236	1.436	0.963	0.507
0.40	0.940	0.923	0.904	0.884	0.787	0.675	0.456
0.60	0.602	0.593	0.584	0.574	0.529	0.478	0.369
1.00	0.331	0.327	0.323	0.319	0.300	0.281	0.239

TABLE IV
DELAY MARGIN $\tau_d \propto K_I$, MULTI-AREA LFC, SIMPLIFIED SINGLE TIME DELAY

	τ_d (s)		
K_I	$\mu = 0$	$\mu = 0.5$	$\mu = 0.9$
0.05	27.8484	23.9877	20.3348
0.10	13.6987	11.7252	9.7542
0.15	8.9743	7.6168	6.1528
0.20	6.6026	5.5501	4.2903
0.40	3.0023	2.3671	1.3830
0.60	1.7452	1.1801	0.7320
1.00	0.5725	0.2247	0.2247

TABLE V
DELAY MARGINS $\tau_d \propto (K_P, K_I)$, $\mu = 0$, MULTI-AREA LFC, SIMPLIFIED SINGLE TIME DELAY

τ_d (s)	K_I						
K_P	0.05	0.1	0.15	0.2	0.4	0.6	1.0
0	27.848	13.699	8.974	6.603	3.002	1.745	0.573
0.05	27.830	14.020	9.205	6.777	3.095	1.810	0.616
0.10	27.001	13.650	9.166	6.881	3.174	1.863	0.649
0.20	25.090	12.702	8.572	6.497	3.209	1.931	0.692
0.40	20.278	10.364	7.014	5.338	2.735	1.731	0.637
0.60	14.228	7.332	4.944	3.768	1.920	1.198	0.443
1.00	0.465	0.455	0.444	0.433	0.384	0.332	0.227

B. Two-Area LFC Scheme

Delay margins are calculated for a two-area LFC scheme based on simplifying multiple delays as one single delay and multiple different delays, respectively. Gains of PI controller of each area are assumed to be equal.

1) Simplified Single Time Delay: At this case, multiple time delays are assumed to be equal with each other, as shown in (8), and the delay margins are calculated based on Theorem 1. At first, delay margins τ_d of the two-area LFC scheme controlled with an I-controller are calculated for constant time delay $(\mu = 0)$ and time-varying delays ($\mu = 0.5$ and $\mu = 0.9$), respectively, as shown in Table IV. The results show that the delay margin of the two-area LFC scheme has similar trend as that of the one-area LFC scheme. The value of the delay margins reduces with the increasing of the value of the gain K_I and the time-varying rate of delays, but with a smaller value for a same gain.

Results about the delay margin of the two-area LFC scheme controlled with a PI controller are summarized in Table V for constant delays $(\mu = 0)$ and Table VI for time-varying delays $(\mu = 0.5)$, respectively. Similar observations can be obtained from those results with that of the one-area LFC system with PI controller.

2) Multiple Different Time Delays: In this case, multiple time delays are treated as unrelated variable, i.e., each area has different delays, as shown in (14). To simply the calculation, only constant delays are considered. The stability region of the

TABLE VI
DELAY MARGINS $\tau_d \propto (K_P, K_I)$, $\mu = 0.5$, MULTI-AREA LFC, SIMPLIFIED SINGLE TIME DELAY

τ_d (s)	K_I						
K_P	0.05	0.1	0.15	0.2	0.4	0.6	1.0
0	23.988	11.725	7.617	5.550	2.367	1.180	0.225
0.05	23.943	12.071	7.870	5.749	2.472	1.252	0.249
0.10	22.926	11.630	7.817	5.835	2.554	1.306	0.269
0.20	20.465	10.421	7.059	5.357	2.534	1.333	0.298
0.40	13.444	7.045	4.802	3.660	1.776	0.887	0.299
0.60	0.848	0.819	0.786	0.750	0.596	0.455	0.258
1.00	0.328	0.320	0.312	0.304	0.272	0.240	0.172

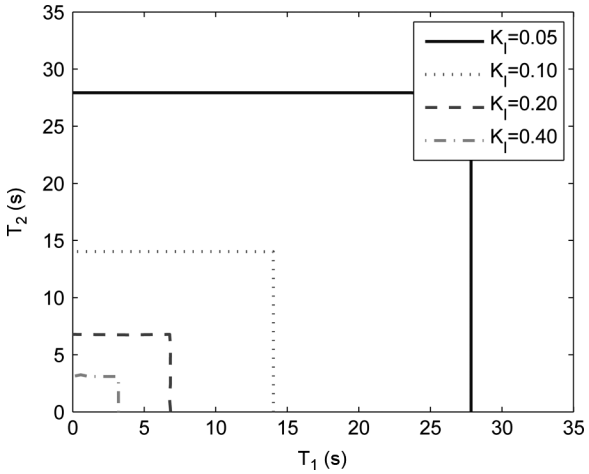

Fig. 7. Stability region of two-area LFC $(K_P = 0.05)$, multiple time delays.

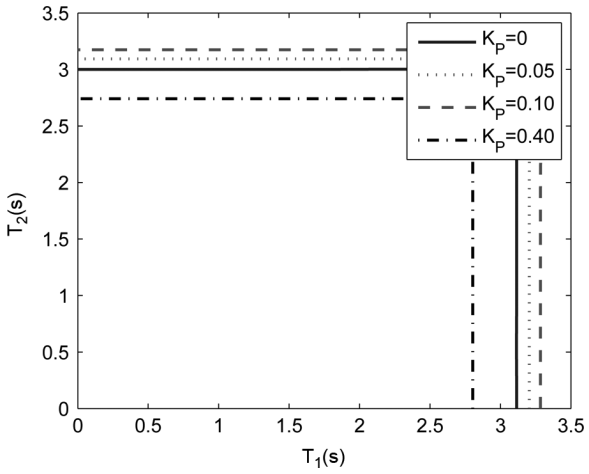

Fig. 8. Stability region of two-area LFC $(K_I = 0.4)$, multiple time delays.

two-area LFC system with two different constant delays is calculated by using Theorem 2. The stability region is a two-dimension region consisting of the delay margin of the two delays. The stability region in (τ_{d_1}, τ_{d_2}) space is shown in Figs. 7 and 8. Some typical points in Figs. 7 and 8 are listed in Table VII, in which the magnitude of two delay margins $|\tau_d|$ and angle θ are defined as $|\tau_d| = \sqrt{\tau_{d_1}^2 + \tau_{d_2}^2}$, $\theta = sin^{-1}(\tau_{d_1}/|\tau_d|)$, respectively.

Results show that for a fixed K_P, as shown in Fig. 7, the delay margin decreases along with the increasing of value of K_I. For a fixed value of $K_I = 0.4$ and with the increasing of the value of K_P, the delay margin increases at first for smaller K_P and then

TABLE VII
DELAY MARGIN $\tau_d \propto (K_I, K_P)$ (TWO-AREA LFC, MULTIPLE TIME DELAYS)

$\|\tau_d\|$ (s)	K_I ($K_P = 0.05$)				K_P ($K_I = 0.40$)			
θ (^{0})	0.05	0.10	0.20	0.40	0	0.05	0.10	0.40
0	27.841	14.029	6.851	3.204	3.114	3.204	3.284	2.803
10	28.270	14.245	6.874	3.254	3.161	3.254	3.334	2.846
20	29.627	14.929	7.274	3.410	3.313	3.410	3.494	2.982
30	32.148	16.199	7.881	3.700	3.595	3.700	3.792	3.236
40	33.987	18.314	8.925	4.184	4.066	4.184	4.288	3.659
45	39.367	19.827	9.586	4.377	4.246	4.377	4.490	3.877
50	36.459	18.306	8.831	4.037	3.917	4.037	4.144	3.579
60	32.250	16.193	7.781	3.571	3.465	3.571	3.665	3.165
70	29.722	14.923	7.181	3.291	3.193	3.291	3.377	2.917
80	28.360	14.240	6.868	3.290	3.047	3.140	3.223	2.784
90	27.930	14.023	6.777	3.093	3.000	3.093	3.173	2.741

reduces for a larger $K_P = 0.4$, which show the similar trend as in the one-area LFC system or the multi-area LFC system simplified as single delay system.

When the delay margins $\tau_{d_1} = \tau_{d_2}$, the corresponding $\theta = 45^0$. From Table VII, for $K_P = 0.05, K_I = 0.2$, it can find that the $|\tau_d| = 9.586$, thus $\tau_{d_1} = \tau_{d_2} = |\tau_d|\sin(45^0) = 6.778s$, which is the same as that obtained from the simplified single delay system, as shown in Table V. In other words, if the τ_1 is assumed to be equal to τ_2, the delay margin obtained from Theorem 1 is the same as that obtained from the Theorem 2. That is to say, the approximate stability region found by the transformed single delay system is very close to the one obtained from original multiple-delay system. With the benefit of reduced calculation load and simplified analysis, thus it is a good choice to apply this method to deal with the LFC system with many control areas or LFC scheme controlled with a higher-order advanced controller such as the robust control in [5] and [8].

C. Three-Area LFC Scheme

Delay margins of a three-area LFC are calculated based on Theorem 2 for both I and PI controllers. Gains of controller of each area are assumed to be equal. Delays for each area are treated as unrelated and independent variable and only constant delay is calculated.

The stability region of the three-area LFC is a three-dimension region consisting of the delay margin of the three delays. The stability regions of I controller $(K_I = 0.05)$ and PI controller $(K_P = 0.2, K_I = 0.05)$ in $(\tau_{d1}, \tau_{d2}, \tau_{d3})$ space are shown in Figs. 9 and 10, respectively. Some typical points in Figs. 9 and 10 are listed in Tables VIII and IX, where the magnitude of three delay margins vector $\vec{\tau}_d$ are defined as $|\tau_d| = \sqrt{\tau_{d_1}^2 + \tau_{d_2}^2 + \tau_{d_3}^2}$, and $\tau_{d_1} = |\tau_d|\sin(\phi)\cos(\theta)$, $\tau_{d_2} = |\tau_d|\sin(\phi)\sin(\theta)$, $\tau_{d_3} = \tau_d \cos\phi$, where ϕ is the angle between the vector $\vec{\tau}_d$ and the axis τ_{d_3}, θ is the angle between the projection of vector $\vec{\tau}_d$ at the plane (τ_{d_1}, τ_{d_2}), and the axis of τ_{d_1}.

The shape of the stability region of two-area LFC scheme looks like a rectangular and the stability region of three-area LFC scheme looks like a cube, which means that the delay margins of different areas are almost unaffected by each other. This phenomenon can be explained by the following two aspects. At first, the couplings between different control areas are low because of the characteristic of the sparse coupling matrices, as indicated by A_{ij} in (5). Secondly, the used Lyapunov-

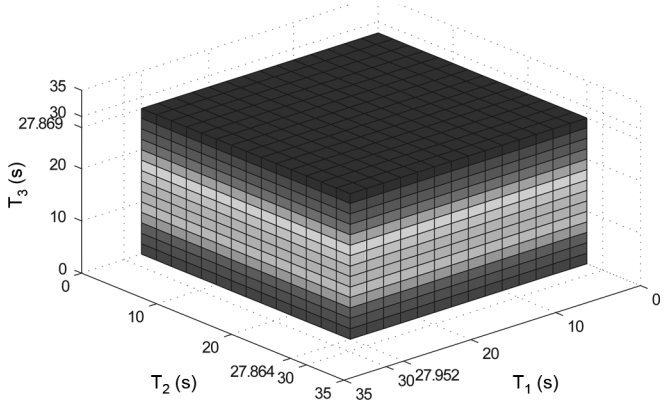

Fig. 9. Stability region of three-area LFC system with a I controller ($K_I = 0.05$).

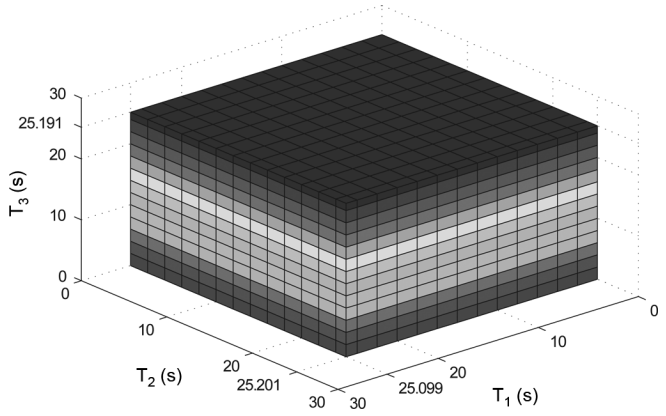

Fig. 10. Stability region of three-area LFC system with a PI controller ($K_P = 0.2, K_I = 0.05$).

TABLE VIII
DELAY MARGIN τ_d (THREE-AREA LFC, MULTIPLE CONSTANT TIME DELAYS)

$\lvert\tau_d\rvert$	ϕ						
θ	0	20	40	45	50	70	90
0	27.869	29.657	36.380	39.413	36.489	29.746	27.952
10	27.869	29.657	36.380	39.413	37.052	30.205	28.383
20	27.869	29.657	36.380	39.413	38.831	31.655	29.746
30	27.869	29.657	36.380	39.413	42.134	34.348	32.276
40	27.869	29.657	36.380	39.413	43.356	38.831	36.489
45	27.869	29.657	36.380	39.413	43.356	41.936	39.407
50	27.869	29.657	36.380	39.413	43.356	38.709	36.375
60	27.869	29.657	36.380	39.413	42.002	34.240	32.175
70	27.869	29.657	36.380	39.413	38.709	31.556	29.653
80	27.869	29.657	36.380	39.413	36.936	30.110	28.294
90	27.869	29.657	36.380	39.413	36.375	29.653	27.864

TABLE IX
DELAY MARGIN τ_d (THREE-AREA LFC, MULTIPLE CONSTANT TIME DELAYS)

$\lvert\tau_d\rvert$	ϕ						
θ	0	20	40	45	50	70	90
0	25.191	26.807	32.884	35.625	32.764	26.709	25.099
10	25.191	26.807	32.884	35.625	33.269	27.121	25.486
20	25.191	26.807	32.884	35.625	34.867	28.423	26.709
30	25.191	26.807	32.884	35.625	37.833	30.840	28.981
40	25.191	26.807	32.884	35.625	39.190	34.866	32.764
45	25.191	26.807	32.884	35.625	39.190	37.773	35.495
50	25.191	26.807	32.884	35.625	39.190	35.008	32.897
60	25.191	26.807	32.884	35.625	37.986	30.966	29.099
70	25.191	26.807	32.884	35.625	35.008	28.539	26.818
80	25.191	26.807	32.884	35.625	33.405	27.231	25.589
90	25.191	26.807	32.884	35.625	32.897	26.818	25.201

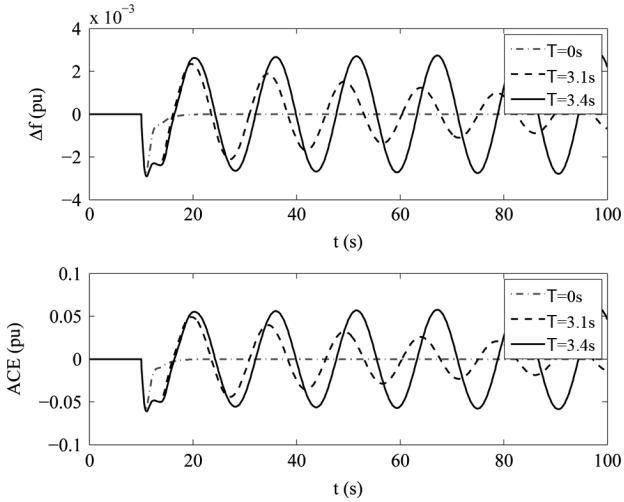

Fig. 11. Time response of one-area LFC ($K_I = 0.4$) with time delays.

based stability criterion is the sufficient condition based and has inevitable conservatism which cannot effectively take into account the low coupling effect between different LFC areas. Further studies should pay attention to reduce the conservatism of the algorithm. On the other side, those findings also indicate that for an LFC scheme with N control area, delay margins can be calculated approximately as N single-area LFC scheme.

D. Evaluation Via Simulation

Simulation studies are carried out to verify the accuracy of delay margin obtained and the effectiveness of the criterion used. This is an alternative way to obtain τ_d approximately by increasing the delay step by step and observing the stability of the system response. To simplify the analysis, only fixed delays and Integrator controller for one-area LFC scheme are verified and reported. The response of LFC scheme equipped with a PI controller ($K_P = 0$, $K_I = 0.4$) under different delays are showed in Fig. 11. At $t = 10s$, a positive load disturbance of 0.1 pu is added to the system. Simulation results show that the delay margin is within the range $[3.1s, 3.4s]$, which is very close to the calculated value 3.1214 s shown in Table I. This result demonstrates the calculation method used has relatively less conservativeness and the results obtained can be used to guide the tuning of the LFC controller.

E. Remarks

- During the design of PI controller for LFC scheme, its gains (K_P, K_I) are mainly determined based on the requirement of the damping performance. Under same circumstance, they have always been chosen as larger as possible to achieve better damping performances. However, after considering of the delay-dependent stability, (K_P, K_I) can be chosen to achieve a trade-off between the damping performance and the delay margin. Moreover, the delay margins obtained can be used as a new performance index and combined with optimization algorithms such as gradient algorithm and genetic algorithm to tune the controller and achieve the online trade-off between delay margin and dynamic performance [27].

- The delay margins obtained can also help the operation of conventional LFC in case of the fault of the communication channels by setting up a bigger upper bound of the communication fault counter. This will extend the on service time of the conventional LFC scheme in case of communication faults.
- For an LFC scheme using open-communication networks, the calculation of the delay margin plays an even more important role as the results obtained from those case studies show that the delay margin reduces sharply with the increasing of the rate of time-varying delays. Thus delay margin should be taken into account at the design stage of the those additional controllers proposed mainly for handling the time-varying delays.
- Note that both the investigation and verification via simulation studies are based on conventional LFC model. Further studies should be based on modeling and simulation of bilateral-based LFC scheme which intends to use the open communication channels.

V. Conclusions

The delay dependent stability of an LFC scheme has been investigated by considering both constant and time-varying time delays resulting from the communication channels. The conventional LFC scheme installed with a PI-type controller has been modeled as a linear system with time delays, and then the delay-dependent stability criterion and LMI techniques have been used to find the delay margins. Case studies are investigated based on one-area LFC scheme with single time delay and multi-area LFC schemes with multiple time delays. Results show that the gains of PI controller are one of the key factors influencing the delay margins. For a fixed proportional gain, the delay margin increases with the decrease of the integral gain of the PI controller. However, for a relatively big fixed integral gain, the delay margin increases at first and then decreases, with the increase of the proportional gain. A small decrement of the controller gains may lead to a significant increment of the delay margin and the delay margin reduces sharply with the increase of the rate of the time-varying delay. Several simplification techniques have been proposed to deal with the multiple time delays of a multi-area LFC scheme. Finally, the effectiveness of the criterion used is verified by the simulation studies which demonstrate that the calculated delay margins are close to its real value.

Delay margin obtained can be used to guide the design and tuning of the controller for LFC scheme so as to achieve compromise between the dynamic performance and the delay margins. The proposed method can be employed to evaluate the delay-dependent stability of LFC scheme equipped with advanced controllers designed specially to deal with the time-varying delays.

Appendix A

The detailed elements of the matrix Ξ in (16) are shown as follows:

$$\Xi_{00} = PA + A^T P + \sum_{i=1}^{n} Q_i + \sum_{j=1}^{n} (N_0^{0j} + [N_0^{0j}]^T) + A^T G A + \sum_{i=0}^{n} \sum_{j=i+1}^{n} (\tau_j - \tau_i) X_{00}^{ij}$$

$$\Xi_{0k} = PA_k - \sum_{i=0}^{k-1} N_0^{ik} + \sum_{i=1}^{n} [N_k^{0i}]^T + \sum_{j=k+1}^{n} N_0^{kj} + A^T G A_k + \sum_{i=0}^{n} \sum_{j=i+1}^{n} (\tau_j - \tau_i) X_{0k}^{ij} \ (k = 1, 2, \ldots, n)$$

$$\Xi_{kk} = -Q_k - \sum_{i=0}^{k-1} (N_k^{ik} + [N_k^{ik}]^T) + \sum_{j=k+1}^{n} (N_k^{kj} + [N_k^{kj}]^T) + A_k^T G A_k + \sum_{i=0}^{n} \sum_{j=i+1}^{n} (\tau_j - \tau_i) X_{kk}^{ij} \ (k = 1, 2, \ldots, n)$$

$$\Xi_{lk} = -\sum_{i=0}^{k-1} N_l^{ik} - \sum_{i=0}^{l-1} [N_k^{il}]^T + \sum_{j=k+1}^{n} N_l^{kj} + \sum_{j=l+1}^{n} [N_k^{lj}]^T + A_l^T G A_k + \sum_{i=0}^{n} \sum_{j=i+1}^{n} (\tau_j - \tau_i) X_{lk}^{ij} \ (l = 1, 2, \ldots, n, l < k \le n)$$

$$G = \sum_{i=0}^{n} \sum_{j=i+1}^{n} (\tau_j - \tau_i) W^{ij}.$$

Appendix B

Parameters of LFC scheme are shown in Table X.

TABLE X
Parameters of LFC Scheme

Parameter	$T_{ch}(s)$	$T_g(s)$	R	D	β	$M(s)$
Area 1	0.3	0.1	0.05	1.0	21.0	10
Area 2	0.4	0.17	0.05	1.5	21.5	12
Area 3	0.35	0.20	0.05	1.8	21.8	12
$T_{12} = 0.1986$ pu/rad,		$T_{13} = 0.2148$ pu/rad,		$T_{23} = 0.1830$ pu/rad		

One-area LFC scheme: Area 1; two-area LFC scheme: Areas 1 and 2; three-area LFC scheme: Areas 1, 2 and 3.

References

[1] P. Kundur, *Power System Stability and Control*. New York: McGraw-Hill, 1994.

[2] F. F. Wu, K. Moslehi, and A. Bose, "Power system control centers: past, present, and future," *Proc. IEEE*, vol. 93, no. 11, pp. 1890–1908, Nov. 2005.

[3] I. P. Kumar and D. P. Kothari, "Recent philosophies of automatic generation control strategies in power systems," *IEEE Trans. Power Syst.*, vol. 20, no. 1, pp. 346–357, Feb. 2005.

[4] K. Tomsovic, D. E. Bakken, V. Venkatasubramanian, and A. Bose, "Designing the next generation of real-time control, communication, and computations for large power systems," *Proc. IEEE*, vol. 93, no. 5, pp. 965–979, May 2005.

[5] S. Bhowmik, K. Tomsovic, and A. Bose, "Communication models for third party load frequency control," *IEEE Trans. Power Syst.*, vol. 19, no. 1, pp. 543–548, Feb. 2004.

[6] D. Rerkpreedapong, A. Hasanovic, and A. Feliachi, "Robust load frequency control using genetic algorithms and linear matrix inequalities," *IEEE Trans. Power Syst.*, vol. 18, no. 2, pp. 855–861, May 2003.

[7] H. Shayeghi, H. A. Shayanfar, and A. Jalili, "Multi-stage fuzzy PID power system automatic generation controller in deregulated environments," *Energy Convers. Manage.*, vol. 47, no. 18, pp. 2829–2845, Nov. 2006.

[8] X. F. Yu and K. Tomsovic, "Application of linear matrix inequalities for load frequency control with communication delays," *IEEE Trans. Power Syst.*, vol. 19, no. 3, pp. 1508–1515, Aug. 2004.
[9] K. Vrdoljak, I. Petrovic, and N. Peric, "Discrete-time sliding mode control of load frequency in power systems with input delay," in *Proc. 12th Int. Power Electronics and Motion Control Conf., EPE-PEMC*, Potoroz, Slovenia, Aug. 2006, pp. 567–572.
[10] H. Bevrani and T. Hiyama, "A control strategy for LFC design with communication delays," in *Proc. 7th Int. Power Engineering Conf.*, Nov. 2, 2005, vol. 2, pp. 1087–1092.
[11] H. Bevrani and T. Hiyama, "Robust decentralised PI based LFC design for time delay power systems," *Energy Convers. Manage.*, vol. 49, no. 2, pp. 193–204, Feb. 2008.
[12] L. Yang *et al.*, "A preliminary study of AGC structure for a regional system considering communication delays," in *Proc. IEEE Power and Energy Soc. General Meeting*, Jun. 2005, pp. 618–623.
[13] H. Bevrani and T. Hiyama, "On load-frequency regulation with time delays: design and real-time implementation," *IEEE Trans. Energy Convers.*, vol. 24, no. 1, pp. 292–300, Mar. 2009.
[14] H. J. Jia and X. D. Yu, "A simple method for power system stability analysis with multiple time delays," in *Proc. IEEE Power and Energy So. General Meeting*, Jul. 20–24, 2008.
[15] N. Olgac and R. Sipahi, "An exact method for the stability analysis of time-delayed linear time-invariant (LTI) systems," *IEEE Trans. Autom. Control*, vol. 47, no. 5, pp. 793–797, May 2002.
[16] R. Sipahi and N. Olgac, "Complete stability robustness of third-order LTI multiple time-delay systems," *Automatica*, vol. 41, no. 8, pp. 1413–1422, Aug. 2005.
[17] Z. Y. Liu, C. Z. Zhu, and Q. Y. Jiang, "Stability analysis of time delayed power system based on cluster treatment of characteristic roots method," in *Proc. IEEE Power and Energy Soc. General Meeting*, Jul. 20–24, 2008.
[18] Y. He, Q. G. Wang, L. H. Xie, and C. Lin, "Further improvement of free-weighting matrices technique for systems with time-varying delay," *IEEE Trans. Autom. Control*, vol. 52, no. 2, pp. 293–299, Feb. 2007.
[19] M. Wu, Y. He, J. H. She, and G. P. Liu, "Delay-dependent criterion for robust stability of time-varying delay systems," *Automatica*, vol. 40, no. 8, pp. 1435–1439, Aug. 2004.
[20] S. Y. Xu and J. Lam, "On equivalence and efficiency of certain stability criteria for time-delay systems," *IEEE Trans. Autom. Control*, vol. 52, no. 1, pp. 95–101, Jan. 2007.
[21] Y. He, M. Wu, and J. H. She, "Delay-dependent stability criteria for linear systems with multiple time delays," *Proc. Inst. Elect. Eng.: Control Theory Appl.*, vol. 153, no. 4, pp. 447–452, Jul. 2006.
[22] W. Yao, L. Jiang, Q. H. Wu, J. Y. Wen, and S. J. Cheng, "Delay-dependent stability analysis of the power system with a wide-area damping controller embedded," *IEEE Trans. Power Syst.*, vol. 29, no. 1, pp. 233–240, Feb. 2011.
[23] H. Bevrani, *Robust Power System Frequency Control*. New York: Springer, 2009.
[24] V. Donde, M. A. Pai, and I. A. Hiskens, "Simulation and optimization of in an AGC after deregulation," *IEEE Trans. Power Syst.*, vol. 16, no. 3, pp. 481–489, Aug. 2001.
[25] K. Vrdoljak, N. Perivc, and I. Petrovivc, "Sliding mode based load-frequency control in power systems," *Elect. Power Syst. Res.*, vol. 80, no. 5, pp. 514–527, May 2010.
[26] W. Tan and Z. Xu, "Robust analysis and design of load frequency controller for power systems," *Elect. Power Syst. Res.*, vol. 79, no. 5, pp. 846–853, 2009.
[27] W. Tan, "Unified tuning of PID load frequency controller for power systems via IMC," *IEEE Trans. Power Syst.*, vol. 25, no. 1, pp. 341–350, Feb. 2010.
[28] P. Gahinet, A. Nemirovski, A. J. Laub, and M. Chilali, *LMI Control Toolbox User's Guide*. Natick, MA: MathWorks, 2000.

L. Jiang (M'00) received the B.Sc. and M.Sc.(Eng.) degrees from Huazhong University of Science and Technology (HUST), Wuhan, China, in 1992 and 1996, respectively, and the Ph.D. degree from the University of Liverpool, Liverpool, U.K., in 2001, all in electrical engineering.

He has been a Lecturer in electrical engineering in The University of Liverpool since September 2007. His research interests include control and analysis of power system and renewable energy.

W. Yao received the B.Sc. degree and the Ph.D. degree in electrical engineering from Huazhong University of Science and Technology (HUST), Wuhan, China, in 2004 and 2010, respectively.

Currently, he is a postdoctoral research fellow in the College of Electrical and Electronics Engineering, HUST. He worked as a visiting researcher in the Department of Electrical Engineering and Electronics, The University of Liverpool, Liverpool, U.K. His research interests include stability analysis and advanced control applications in power systems.

Q. H. Wu (M'91–SM'97–F'11) received the M.Sc.(Eng.) degree in electrical engineering from Huazhong University of Science and Technology (HUST), Wuhan, China, in 1981; and the Ph.D. degree in electrical engineering from The Queen's University of Belfast (QUB), Belfast, U.K., in 1987.

He has been the Chair of Electrical Engineering in the Department of Electrical Engineering and Electronics, The University of Liverpool, Liverpool, U.K., since September 1995. Since then, he has been the Head of Intelligence Engineering and Automation Research Group working in the areas of systems control, computational intelligence, and electric power and energy.

Prof. Wu is a Chartered Engineer and a Fellow of IET.

J. Y. Wen received the B.S. and Ph.D. degrees in electrical engineering from Huazhong University of Science and Technology (HUST), Wuhan, China, in 1992 and 1998, respectively.

He is a Professor at HUST. He was a Postdoctoral Researcher with HUST from 1998 to 2000, and the Director of Electrical Grid Control Division, XJ Relay Research Institute, Xuchang, China, from 2000 to 2002. His research interests include evolutionary computation, intelligent control, power system automation, power electronics, and energy storage.

S. J. Cheng (M'86–SM'87–F'11) received the B.Sc. degree from Xi'an Jiaotong University, Xi'an, China, in 1967, the M.Eng. degree from Huazhong University of Science and Technology (HUST), Wuhan, China, in 1981, and the Ph.D. degree from the University of Calgary, Calgary, AB, Canada, in 1986, all in electrical engineering.

He has been a Professor at HUST since 1991. His research interests are power system control, stability analysis, application of artificial intelligence, and energy storage.

Prof. Cheng has been a Fellow of the Chinese Academy of Sciences since 2007.